Hydroelastic theory for floating plates of variable flexural rigidity

Simone Michele, University of Plymouth, Drake Circus, Plymouth PL4 8AA, UK, simone.michele@plymouth.ac.uk
Siming Zheng, University of Plymouth, Drake Circus, Plymouth PL48AA, UK, siming.zheng@plymouth.ac.uk
Emiliano Renzi, Northumbria University, UK, emiliano.renzi@northumbria.ac.uk
Alistair Borthwick, University of Plymouth, Drake Circus, Plymouth PL4 8AA, UK, alistair.borthwick@plymouth.ac.uk
Deborah Greaves, University of Plymouth, Drake Circus, Plymouth PL4 8AA, UK, deborah.greaves@plymouth.ac.uk

INTRODUCTION

We present a theoretical model of the hydrodynamic behaviour of a floating flexible plate of variable flexural rigidity connected to the seabed by a spring/damper system. Decomposition of the response into natural modes allows us to investigate the hydroelastic behaviour of the plate subject to monochromatic incident free-surface waves. We show that spatially dependent plate stiffness affects the eigenfrequencies and modal shapes, with direct consequences on plate dynamics. We also examine how plate length and Power Take-Off distribution affect the response of the system and its consequent absorbed energy. This work highlights the need to improve existing models of flexible floating platforms, expecially given their importance in coastal and ocean engineering.

1. MATHEMATICAL MODEL

Figure 1 depicts a two-dimensional floating elastic plate of length $2L$. A Cartesian reference system is defined with x-axis coincident with the undisturbed free-surface level and z-axis pointing vertically upward from still water level. The plate is connected to the rigid seabed z=-h through vertical cables located at $x = x_i$, i=1,...,I. Each cable has constant stiffness, k_{PTO} and damping coefficient, υ_{PTO}. We assume the thickness of the plate to be much smaller than its length, in which case the elastic vibration of the floater can be described by the following Euler-Bernoulli dynamic equation

$$(DW_{xx})_{xx} = q - \mu W_{tt} \quad (1)$$

where W is the plate vertical displacement, t denotes time, q is the transverse distributed load, $D(x)$ is the spatially dependent flexural rigidity, and μ is the constant mass per unit length of the plate.

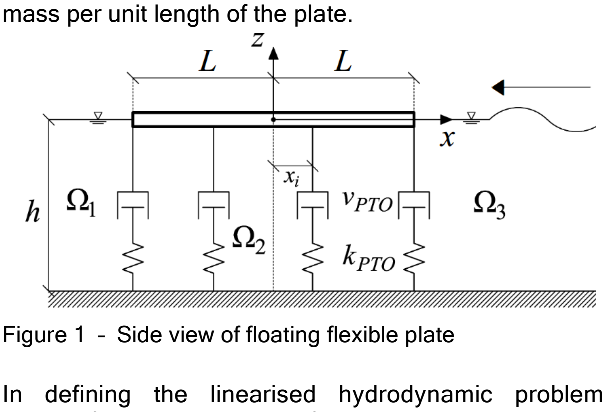

Figure 1 - Side view of floating flexible plate

In defining the linearised hydrodynamic problem, inviscid fluid and irrotational flow are assumed, such that the velocity potential Φ satisfies Laplace's equation in the fluid domain. At the free surface, we apply the following kinematic and mixed boundary conditions

$$\zeta_t = \Phi_z,\ \Phi_{tt} + g\Phi_z = 0,\ z = 0,\ |x| > L \quad (2)$$

where ζ is free-surface elevation and g is acceleration due to gravity. In addition, we require the fluid velocity to be tangential to the seabed, such that $\Phi_z = 0$ in z=-h. By using the thin-plate approximation, the kinematic boundary condition at the wetted surface of the plate reads

$$\Phi_z = W_t, z = 0, x \in [-L, L], \quad (3)$$

Following Newman (1994) and Michele (2022,2023), we assume harmonic motion of frequency ω and decompose the displacement of the plate into a set of rigid (heave and pitch) and elastic dry bending modes, i.e., in the absence of fluid or added mass. Here, we focus on the solution of (1) for stepped variations in D. Natural modes are found using a matching method technique, and Fourier series expansion is used to solve the hydrodynamic problem. The procedure is not reported here for brevity. The dynamic equation (1) in presence of all external forces is

$$(DW_{xx})_{xx} + \mu W_{tt} = -\rho\Phi_t - \sum_i (W_t v_{PTO} + W k_{PTO})\delta(x - x_i) \quad (4)$$

where ρ is fluid density. The first term on the r.h.s. represents the dynamic pressure exerted by the wave field, the second term represents the hydrostatic pressure due to plate displacements, and the third term denotes the stiffening and damping effects of localized forces due to the PTO and mooring system, with δ denoting the Dirac Delta function. Solution of equation (4) gives the complex amplitude of each natural mode and can be found by using orthogonality property of eigenmodes. Given the plate shape, the average power generated is simply

$$P = \frac{1}{2} v_{PTO} \omega^2 \sum_i |w(x_i)|\text{^}2 \quad (5)$$

where $w(x_i)$ represents the complex plate oscillations at PTO location. The system efficiency is given by the capture width ratio $C_W = P/(EC_g)$, where E is total energy and C_g is group velocity.

2. RESULTS AND DISCUSSION

In this section we examine the effects of plate flexural rigidity, plate geometry, PTO system, and wave frequency on the hydrodynamic behaviour and energy extraction efficiency of the floating plate. For simplicity, let us consider a plate system with the following fixed parameters: A = 1 m, h = 10 m and ρ = 1000 kg m^{-3}.

2.1 Effect of plate length

We first examine the effect of plate length on the response of the hydroelastic plate on power extraction efficiency. Two plate lengths, L = [5; 20] m, are considered. Here we assume flexural rigidity $D = \overline{D}$ = 6.9 × 10^4 kg m^3 s^{-2} and μ = 44 kg/m. Furthermore, the stiffness coefficient $k_{PTO} = 0$ and the PTO system comprises seven equally spaced PTO devices. Figure 2 shows the surface plot of C_W as a function of incident wave frequency and PTO coefficient for two different plate lengths. For the smallest plate length, C_W has a single peak not far from the first corresponding eigenfrequency ω = 1.62 rad s^{-1}. As the plate lengthens to 20 m additional secondary peaks develop. This is mainly due to the increased number of eigenfrequencies in the range of interest which are located very close to each other.

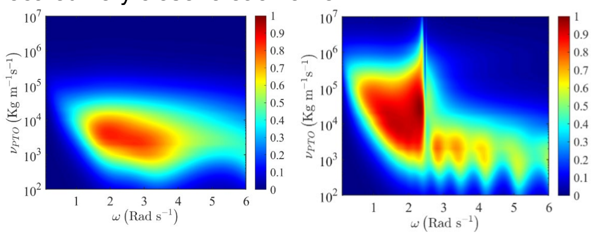

Figure 2 – Capture width ratio as a function of incident wave frequency ω and PTO coefficient for seven equally spaced PTO devices located at x_i = ±[0, L/3, 2L/3, L] and plate lengths of: (a) L = 5 m; and (b) L = 20 m

2.2 Effect of PTO system

We now investigate the influences of PTO coefficient and distribution on power extraction efficiency for a plate of length L = 20 m and $k_{PTO} = 0$. Flexural rigidity and mass per unit length are unchanged. Figure 3(a) refers to two PTO devices located at the plate edges, whereas Figure 3(b) corresponds to nine equally spaced PTO devices. As the number of PTOs increases, the bandwidth of C_W also increases and the system becomes more efficient

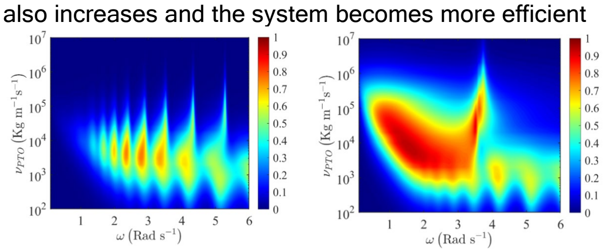

Figure 3 – Capture width ratio as a function of incident wave frequency ω and PTO coefficient for four distributed PTO systems: (a) $x_i = \pm L$; and (c) x_i = ±[0, L/4, L /2, 3 L /4, L]

2.3 Effect of plate flexural rigidity

In this section we investigate the effect of flexural rigidity distribution on power extraction efficiency. We consider a plate made of 3 segments each of length 2L/3 and constant D_m, m = 1, 2, 3. The plate has length L = 20 m, $k_{PTO} = 0$, and possesses 7 equally spaced PTO devices. Figure 4 shows the C_W map with respect to incident wave frequency and PTO coefficient for various distributions of flexural rigidity. Figure 4(a) refers to a plate with a stiff middle segment, $D_m=\overline{D}\times$[0.1, 10, 0.1], whereas Figure 4(b) refers to the opposite case of a plate with stiff ends $D_m = \overline{D}\times$[10, 0.1, 10]. The plate with softer ends exhibits greater efficiency and smoother behaviour of C_W. This highlights a detrimental property of rigid plates with respect to power extraction. Figure 4(c) concerns a case where the plate flexural rigidity increases towards the plate front, such that $D_m=\overline{D}\times$[0.1, 1, 10]. The efficiency is rather poor because the plate enhances wave radiation as $x\to-\infty$. Conversely, Figure 4(d) shows the map obtained for D increasing towards $x = -L$ such that $D_m=\overline{D}\times$[10, 1, 0.1]. This case achieves much greater efficiency, with the map also containing several additional peaks at high frequencies.

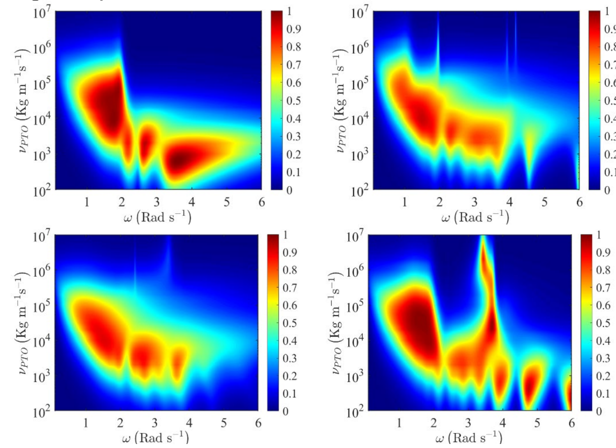

Figure 4 – Capture width ratio as a function of incident wave frequency ω and PTO coefficient for the following stepped variations in D: $D_m = \overline{D}\times$ (a) [0.1, 10, 0.1]; (b) [10, 0.1, 10]; (c) [0.1, 1, 10]; and (d) [10, 1, 0.1];

Given that flexural rigidity plays a similarly important role as PTO distribution, Figure 5 presents capture width ratio maps for uniform plates with different values of D. Figure 5(a) concerns a softened plate with $D = 10^{-2}\times\overline{D}$, and shows that as D decreases, the efficiency of the system increases. Figure 5(b) refers to a rigid plate; in this case there are no contributions from the bending modes and the dynamics is governed by pitching and heaving motion only. The overall efficiency is much lower than in the previous cases because of the smaller number of eigenfrequencies and possible modal optimisations. This highlights the beneficial effect of bending elastic modes on power extraction efficiency.

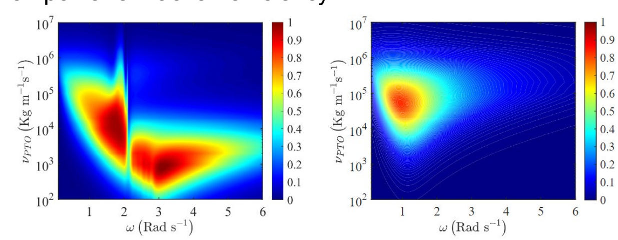

Figure 5 – Capture width ratio as a function of incident wave frequency ω and PTO coefficient for the following constant values of D: (a) $D = 0.01\times\overline{D}$; and (b) Rigid plate.

REFERENCES

1) Newman (1994): Wave effects on deformable bodies. Appl. Ocean Res.16, 47-59.
2) Michele, Zheng, Greaves (2022): Wave energy extraction from a floating flexible circular plate. Ocean Eng. 245, 110275.
3) Michele, Zheng, Buriani, Borthwick, Greaves, (2023): Floating hydroelastic circular plate in regular and irregular waves. Eur. J.Mech. B Fluids 99, 148-162.